Research article

Safety of oral administration of high doses of ivermectin by means of biocompatible polyelectrolytes formulation

Rafael R.M. Madrid [a], Patrick D. Mathews [a,*], Ana C.M.F. Patta [a], Anai P. Gonzales-Flores [b,c], Carlos A.B. Ramirez [a], Vera L.S. Rigoni [a], Marcos Tavares-Dias [d], Omar Mertins [a,**]

[a] Laboratory of Nano Bio Materials (LNBM), Department of Biophysics, Paulista Medical School, Federal University of Sao Paulo (UNIFESP), 04023-062 Sao Paulo, SP, Brazil
[b] Post-Graduate Program in Tropical Biodiversity, Federal University of Amapá, 68903-419 Macapá, AP, Brazil
[c] Institute of Research of the Peruvian Amazon (IIAP, AQUAREC), 17000 Puerto Maldonado, Peru
[d] Embrapa Amapá, 68903-419 Macapá, AP, Brazil

ABSTRACT

The FDA-approved drug ivermectin is applied for treatments of onchocerciasis and lymphatic filariasis. The anti-cancer and anti-viral activities have been demonstrated stressing possibilities for the drug repurposing and therefore new information on high dosage safety is on demand. We analyzed *in vivo* tissue responses for high doses of ivermectin using *Corydoras* fish as animal model. We made intestinal histology and hematologic assays after oral administration of ivermectin transported with polyelectrolytes formulation. Histology showed any apparent damage of intestinal tissues at 0.22–170 mg of ivermectin/kg body weight. Immunofluorescence evidenced delocalization of Myosin-Vb at enterocytes only for the higher dose. Hematology parameters showed random variations after 7 days from administration, but a later apparent recover after 14 and 21 days. The study evaluated the potential of high doses of oral administration of ivermectin formulation, which could be an alternative with benefits in high compliance therapies.

1. Introduction

The application of known drugs, which have been lengthy used with success for specific treatments, for novel usages and in new and emergent diseases, is an actual demand [1, 2]. As a matter of fact, due to the increasing worldwide poverty, the access to new and expensive drugs and treatments becomes restrictive, leading the drug repurposing as an emergent and sustainable alternative [1, 2]. However, for efficient drug repurposing, the knowledge on safety of high dosage, new formulations and ways of administration is highly required.

The current sanitary emergency related to COVID-19 has flurried worldwide seeking of therapies using well-known drugs. In this context, the antiparasitic drug ivermectin, approved by the FDA for the treatment of onchocerciasis and lymphatic filariasis, was recently described to inhibit the causative virus SARS-CoV-2, providing *in vitro* antiviral action with a single dose which was able to control viral replication within 24–48 h [3]. However, in this recent and promising antiviral study, a relative high dose of ivermectin was used and therefore, more

information on high dosage safety would be urgent. Actually, a number of molecular mechanisms of action of ivermectin have been discovered [4, 5], and thereby ivermectin formulations are as well under research for possible applications in cancer therapies and in diseases caused by several RNA viruses such as HIV-1, dengue, influenza, respiratory syndrome virus (RSV) and rabies [6]. In terms of anti-cancer activity, Drinyaev *et al.* [7] have previously shown the ivermectin ability to reduce *in vivo* tumor growth by 50% at day 5 at dose of 1 mg/kg in male mice bearing a solid Ehrlich carcinoma. For the same dose, it was additionally shown the growth inhibition of the carcinoma cell line 755 (C57/BL6 male mice). The administration after vincristine in the Ehrlich carcinoma further evidenced that ivermectin boosted the antitumor effect of vincristine [7], which may be related to the inhibition action of ivermectin on *P*-glycoprotein in the multidrug resistance cells [8]. These studies are few examples of the promising therapeutic effects of ivermectin, stressing the possibilities of repurposing.

As a matter of fact, ivermectin is an especially interesting drug due to the low toxicity in humans and in majority of mammalian [5]. To date, it

---

* Corresponding author.
** Corresponding author.
E-mail addresses: patrickmathews83@gmail.com (P.D. Mathews), mertins@unifesp.br (O. Mertins).

has been largely applied with success as broad-spectrum anti-parasitic drug in human and veterinary medicine [9]. During the past two decades, ivermectin has produced sales over 1 billion USD/year and is annually taken by 250 million people [9, 10].

The oral drug administration is well known for the high compliance and ease of administration, and it is so far the only approved for ivermectin in humans [11]. In the treatment of onchocerciasis, the approved dose of ivermectin is 0.15 mg/kg, but the frequency of administration is still controversial and the duration of treatment has not been established [12]. With the aim to provide more information on means for its safe administration, besides preventing future drug resistance, evidently the evaluation of adequate dosages is equally an actual demand. In terms of gastrointestinal side effects of the currently approved doses of ivermectin, cases of anorexia, constipation, diarrhea, nausea, vomiting and abdominal distention were reported. Hematologic side effects have included decreased leukocyte count, eosinophilia, increased hemoglobin, hematomatous swellings associated with prolonged prothrombin times, leukopenia and anemia [13].

Considering that some gastrointestinal and hematological side effects have been described in humans after administration of the conventional doses of ivermectin, the usage of larger amounts of the drug for possible repurposing requires further information on tolerability and safety. Since the intestinal tract is a region of absorption of the drug after oral administration, the safety of the intestinal tissues needs to be assessed after high dosage administration. Likewise, the hematologic conditions are required and the same can provide important information on the high dosage toxicity. However, little is known in terms of ivermectin interaction and alterations in intestinal tissues and blood cells after oral administration of higher doses, mainly because such studies in humans are difficult to perform or rather impossible. Thereby, the studies using different animal models are crucial. In our recent studies we described the physicochemical and *in vivo* mucoadhesive characteristics of a drug formulation produced with chitosan-*N*-arginine and alginate polyelectrolytes incorporating ivermectin [14]. In the present contribution, we aimed to evaluate the histological effects in intestinal tissues and hematological variations after the oral administration of relative high doses of ivermectin by means of the drug carrier in ornamental fish *Corydoras schwartzi* as *in vivo* animal model. The aim of this study was to contribute to the exploration of dosage possibilities for expanded applications of this drug.

2. Materials and methods

2.1. Production of ivermectin-polyelectrolytes powder formulation

The powder formulation for oral administration was produced by titration as previously described [14]. Briefly, the lyophilized powder of chitosan-*N*-arginine (CHarg; Mw: 135 kDa; DDA: 95%; DS: 3.5%) was dissolved in acetate buffer (80 mM, pH 4.50 ± 0.02) at 1 mg/mL by vortex mixing for 3 min then submitted to bath sonication (40 kHz, 25 °C; Eco-Sonics Q3.0L, Brazil) for 30 min; ivermectin concentrations (22, 23-dihydroavermectin, 99%; Ivermectan, UCBVET, Brazil) varying from 0.4 to 38 μM were included for drug-containing preparations and the procedure was repeated plus keeping the solutions under stirring overnight (800 rpm); alginate (200 kDa; Sigma-Aldrich) solution was prepared in the same manner at 0.1 mg/mL. The alginate solution was titrated at 2 mL/min into CHarg or CHarg/ivermectin solutions under stirring (1200 rpm) and after the mixtures were kept under stirring overnight at 22 ± 1 °C. The colloidal dispersions were centrifuged (Sorvall Super T21 Centrifuge; Newtown, CT) at 21000 rpm and 4 °C for 25 min. The supernatants were removed, and new equivalent volumes of pure water (pH 6.5) were added to the pellets, which were newly dispersed by vortex mixing (3 min); this procedure was repeated three times. Following, all centrifuged samples were lyophilized (Liotop, Liobras, Brazil) during 48 h and then saved in a refrigerator at 4 °C until use. The collected supernatants of each centrifugation were diluted to equal

volumes of methanol in order to solubilize eventual residual of ivermectin not incorporated to the particles and the absorbance was read at 246 nm (Ultrospec 8000 UV-Vis Spectrophotometer, Cytiva Elements, USA) to detect the presence of free ivermectin [15]. Since the absorbance of the supernatant of each ivermectin-containing preparation was negligible as the absorbance of the preparation without ivermectin, it was confirmed that the totality of drug was incorporated in the micro hydrogel particles.

2.2. Scanning electron microscopy (SEM)

The obtained powder formulations were analyzed with SEM at Electron Microscopy Center (CEME) at UNIFESP. The samples were prepared by lightly sprinkling the freeze-dried powders on a double side adhesive carbon tape, which already stuck on aluminum stubs. The stubs were then placed into fine coat ion sputter (Leica EM SCD 500, Germany) and metalized by sputtering with platinum. The samples were exposed to accelerate voltage beam with strength of 20.0 and 30.0 kV, then randomly scanned for particle size and surface morphology. SEM micrographs at different magnifications were captured on a Field Emission Gun FEI Quanta FEG 250 microscope.

2.3. In vivo experiments

In vivo experiments were performed following our previous protocols [14, 16] using *Corydoras schwartzi* fish, bought from commercial provider, employing three aquariums of 15 L, one for the control group, one for the 0.22 mg/kg ivermectin dose and one for the 0.86 mg/kg ivermectin dose. Fish were placed in the aquariums with dechlorinated water, previously conditioned to adequate water conditions for the species, with a constant temperature using thermostat systems (Hopar Aquarium Heater H-606 150W, China), constant pH and adjusted physicochemical parameters (Seachem Prime water conditioner, Madison, GA, USA) and submitted to constant filtration and aeration (Aquatech FE25 Filtration System, China) with the water flow rate adjusted to 250 L/h. Fish were nourished with commercial ration TetraMin (Tetra GmbH, Germany), adequate for ornamental fish, twice a day (8 AM and 6 PM) and monitored for seven days. Each aquarium had equal amount of 50 individuals (n = 50). A 12 h light/dark cycle was adopted in the aquariums room. Fish where kept in 12 h fasting before experiments. To each aquarium, the same amount of lyophilized powder free of ivermectin or containing a specific concentration of ivermectin was dispersed in the aquarium water after the filtration system was turned off in order to avoid particles retention. All fish avidly fed on particles (see illustrative video at [17]). At day 7, 7 fish from each aquarium were individually and randomly collected with appropriate collecting net for hematology and histology as described bellow. At days 14 and 21 the same collecting of 7 fish from each aquarium was performed. All fish were weighted and ivermectin doses were calculated considering the concentration in the administrated weight of particles and the average fish body weight from the corresponding aquarium; thus, the doses were expressed as averages in mg of ivermectin per kg of fish body weight. In total, 42% of the population of each aquarium was examined. A second experiment was performed to evaluate the 170 mg/kg ivermectin overdose employing smaller aquarium of 4 L where 5 fish were acclimatized 72 h before the experiment. The 5 fish were equally examined between 15 and 20 min following the administration, time when the first physical alterations due to overdose were perceived. This experiment was performed in triplicate and the averages and standard deviations of hematology data were calculated for the total of analyzed fish (n = 15), representing 100% of the population. The protocols carried out during *in vivo* studies were approved by the Animal Ethical Committee of the Federal University of Sao Paulo and all experiments were performed in accordance with the U.K. Animals Scientific Procedures Act, 1986 and associated guidelines, EU Directive 2010/63/EU for animal experiments, and the National

Institute of Health guide for the care and use of Laboratory animals (NIH Publications No. 8023, revised 1978).

2.4. Hematology parameters

Blood samples were collected by puncture of the caudal vessel, using 0.3 mL syringe for insulin (Becton Dickinson) containing 10% of ethylene diamine tetra-acetic acid (EDTA). Erythrocyte counts (RBC) were conducted in a Neubauer chamber (Blaubrand) after dilution in formalincitrate solution and blood smears were prepared and stained with May-Grünwald Giemsa-Wright [18, 19]. Subsequently, these were used for leukocyte and total thrombocyte counts, and for leukocyte differential counts [20]. Statistic analyses were performed using ANOVA and Student's t-test.

2.5. Histology of intestine

Immediately after blood collection, the fish were euthanized by neural pithing [21]. In necropsies the intestines were removed and fixed in 10% buffered formalin solution, dehydrated in increasing series of ethanol, diaphanized, embedded in paraffin, cut into serial sections 4 µm thick using a Leica RM2255 automated microtome, and stained with hematoxylin-eosin (H&E) [22] and periodic acid-Schiff (PAS) [23]. Images were captured using a Leica DM 1000 microscope coupled to a computer and using the Leica Application Suite software version 1.6.0 for image capture. Immunostaining was carried out in 4 µm tissue sections, after deparaffination and antigen retrieval with 10 mM citrate buffer (pH 6.0) in a pressure cooker for 4 min [24]. The antibody anti-MYO5B (1:200 dilution; Santa Cruz Biotechnology Inc.) was used following the manufacturer instructions. The samples were counterstained with DAPI (4′,6-diamidino-2-phenylindole dihydrochloride; Sigma Aldrich) for visualizing nuclei. Samples were examined in a Confocal Leica TCS SP8 Inverted Microscope, using $10\times$, $40\times$, $63\times$ and $100\times$ objectives. The fluorescent dyes were excited with a diode-pumped solid-state laser and the Leica Application Suite X was used for image capture and analysis.

2.6. Statistical data analyses

Results were expressed as mean and standard deviation. The analysis of variance (ANOVA) was used. When there were significant differences between the groups, the Dunnett test and Student-t test were used to compare each treatment with the control using the statistical software "Sigma Plot 11".

3. Results and discussion

3.1. Formulation and in vivo administration

The micro hydrogel drug carrier free of ivermectin or containing ivermectin (Figure 1a) was produced by titration and freeze dried [14]. The obtained powder form was analyzed using SEM (Figure 1b). It evidences particulate structures of irregular and globular shapes with slightly rough surface, but an overall submicrometric size distribution. The powder was fed to *Corydoras* fish in systematic experiments consisting the evaluation of the control (free of drug) and the drug concentrations of 0.22, 0.86 and 170 mg/kg of body weight (b.v.). The control and the two lower drug concentrations were performed in a three weeks study (total 21 days), but the higher concentration, which represents a lethal dose to fish, was performed in triplicate assay as described in 2.3.

The polyelectrolytes formulation consists an effective carrier for hydrophobic molecules as ivermectin [14, 16]. Indeed, both main components, *i.e.*, chitosan and alginate have shown excellent characteristics for applications in drug delivery materials [25, 26, 27]. Since both macromolecules are weak polyelectrolytes, the charge balance between COO^- and NH_3^+ groups, which are pH-dependent, triggers structure characteristics as well the interaction with the biological media [14, 16]. Similar

features have been reported in compact polyelectrolyte complexes of poly(methacrylic acid)/poly(allylamine hydrochloride) [28, 29] for
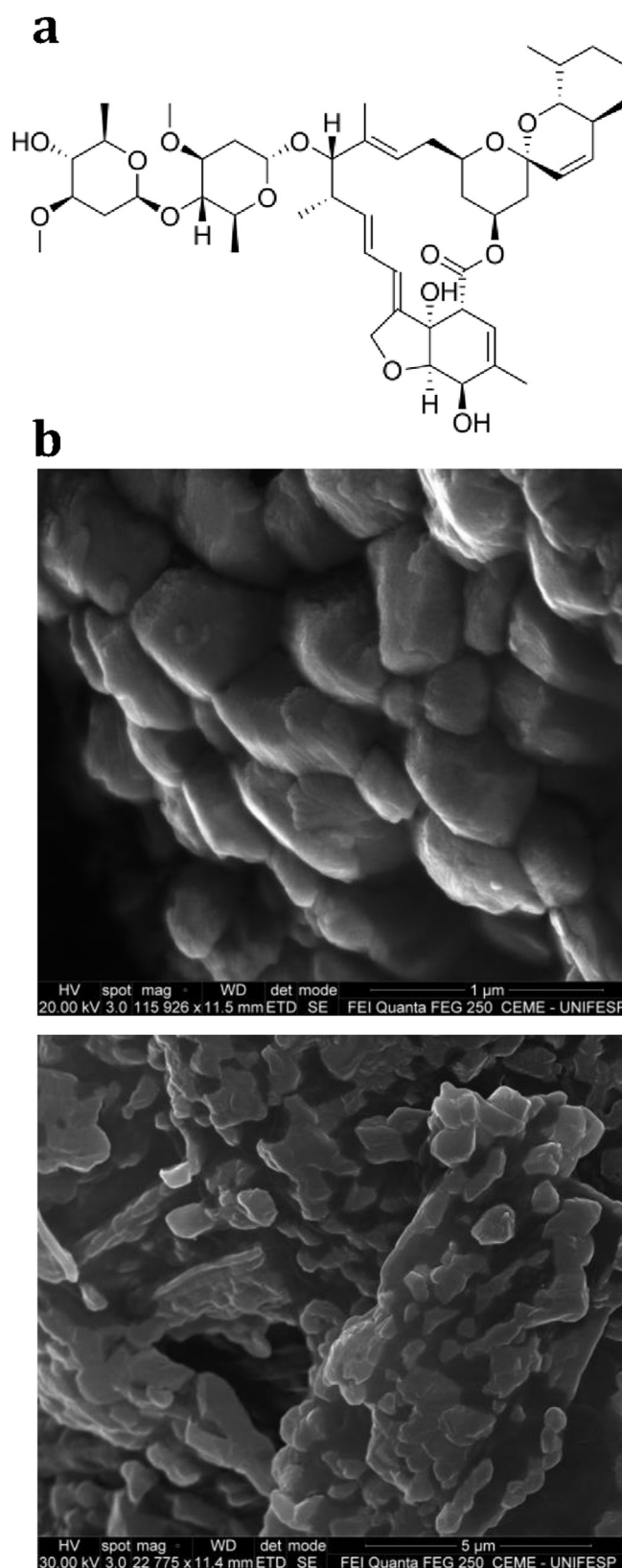
Figure 1. Molecular structure of ivermectin (a). Scanning electron microscopy (SEM) of freeze-dried ivermectin-polyelectrolyte formulation evidencing irregular submicrometric particles with wrinkled surface (b).

which the destabilization of the charge balance leaded changes in their properties at multiple scales, including microstructure and mechanical features. For our micro hydrogel particles formulation, when pH rises and the environment becomes moderately alkaline as in the intestinal tract (pH = 7.8), a transition from mass to surface fractal was observed, leading to structures with rough surfaces where the interface between particles and the surrounding medium is diffuse [14]. With this characteristic the mucoadhesiveness and retention of the particles was identified in the intestines of *Corydoras schwartzi*, denoting the profitable interaction of the particles with the expected site of drug delivery [14].

As previously revealed, the powder formulation provides as well high compliance to the fish, which avidly consume the material immediately after throwing it in the aquarium (see video at [17]). After consumption, the drug absorption is evidenced by the concentration dependent toxicity of ivermectin, which is known neurotoxic to fish as it crosses the blood brain barrier blocking neuro-transmitters by acting on GABA-gated Cl⁻ channels [30]. The neurotoxicity lead to apparent physical alterations like skin darkening, downrolling of the eyes, lethargy and mortality. Actually, a mortality of 28% was produced for the lower 0.22 mg/kg b.v. and 32% for the 0.86 mg/kg. The mortality was always observed during the first 24 h after administration. The dose of 170 mg/kg was an exceptional lethal dose, which leads fish to dead between 30 and 45 min after administration. The fish from the overdose were examined immediately when the first physical or behavior alterations were perceived, usually between 15 and 20 min after administration. No mortality and any fish characteristic or behavior alteration were observed for the control group.

3.2. Intestines histology

Since ivermectin is currently applied by oral administration, the alterations in intestinal tissues related to higher dosage, which may be required for possible drug repurposing, are important issues to evaluate the intestinal feasibility or tolerance to the higher dosage. In the event of tissues damage and toxicity, a specific dosage can be unliked to further studies and application. In this study, three techniques of histology were performed with several intestinal tissues from all the different protocols of ivermectin administration, *i.e.*, 0.22, 0.86 and 170 mg/kg b.w. Figure 2 and Figure S1 show representative photomicrographs of the intestinal tissues. The thorough search for tissue damage revealed any apparent alteration on the surface of the intestinal mucosa, neither on internal and submucosal layers in examining several H&E and PAS histologic sections of the whole intestinal tract. Comparing the control group with the different ivermectin concentrations groups, the histology evidenced any erosion, abrasion, hyperplasia, necrosis and neither the presence of inflammatory cells, unveiling the absence of morphologic alterations.

The only exceptional alteration was found in histology analysis of the immunofluorescence of Myosin-Vb for the ivermectin overdose, *i.e.*, 170 mg/kg b.w. Myosin-Vb is a protein of the unconventional class V myosin family that is, along with its interacting proteins Rab11 and Rab8, involved in the transport of cytoplasmic vesicles in epithelial cells [31, 32, 33, 34]. It has been further reported that Myosin-Vb regulates localization of apical proteins toward the plasma membrane [35, 36]. In examining the immunofluorescence, we observed an increase in Myosin-Vb staining at apical regions of enterocytes (Figure 2c) indicating that ivermectin resulted in increased expression of the Myosin-Vb at those apical regions. In polarized epithelial cells of intestinal enterocytes [37], the synergistic between Rab11a and the actin-based motor Myosin-Vb plays a crucial role in the regulation of apical trafficking [38], hence Myosin-Vb has an essential role in maintaining the epidermal barrier integrity. The characterized overexpression indicates that Myosin-Vb is affected by the high concentration of
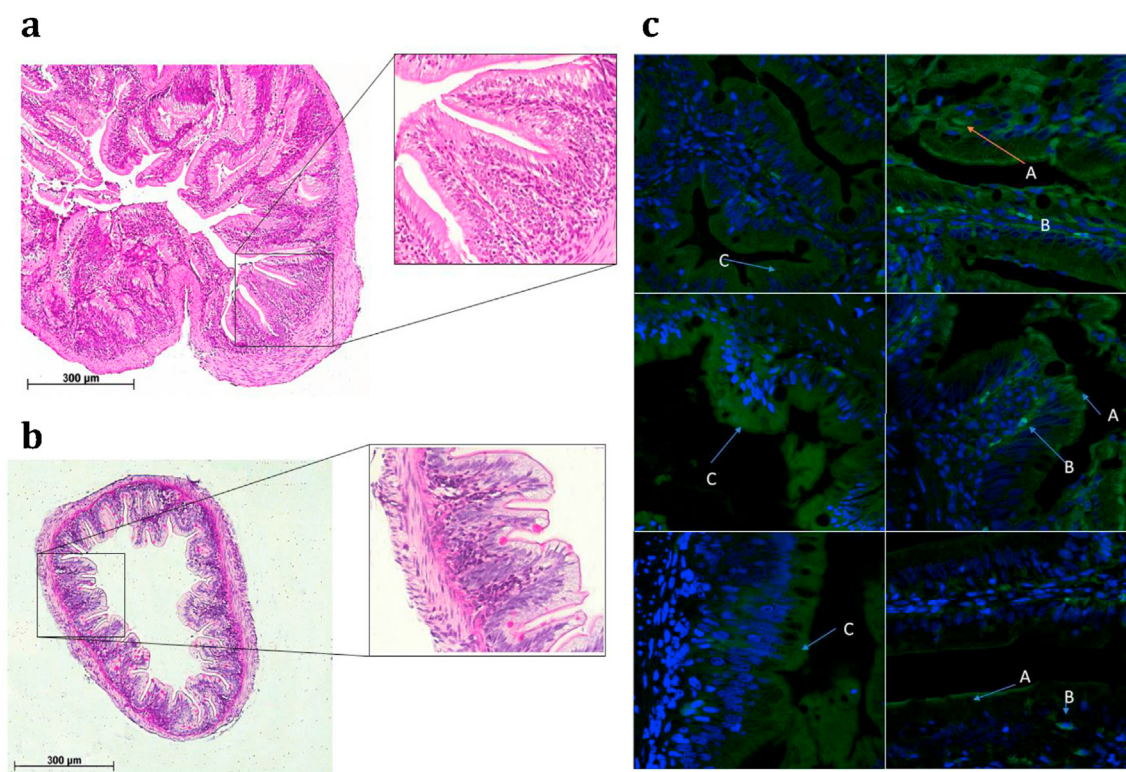

Figure 2. Intestine histology of *Corydoras schwartzi* photomicrographs with Hematoxylin-eosin (a) and PAS (b) staining showing absence of alteration after administration of ivermectin formulations, and immunofluorescence of Myosin-Vb expression (c) comparing control sections (left) to sections from the ivermectin overdose (right). A and B show examples of regions with increased fluorescence of Myosin-Vb, and C shows even distribution of fluorescence (Myosin-Vb: FITC-green; nuclei: DAPI-blue).

Table 1. Blood cells parameters of *Corydoras schwartzi* after administration of 0.22 and 0.86 mg/kg ivermectin during 7, 14 and 21 days compared to the control. Data are expressed as mean ± standard deviation.

Time	Parameters	Ivermectin concentration (mg/kg)		
		Control	0.22	0.86
7 days	RBC (x10^6 μL^{-1})	0.20 ± 0.05[a]	0.20 ± 0.06[a]	0.11 ± 0.06[a]
	Thrombocytes (μL)	17,775 ± 6865[a]	15,660 ± 2823[a]	14,310 ± 8284[a]
	WBC (x10^3 μL^{-1})	12,667 ± 4475[a]	129,204 ± 104,411[b]	58,590 ± 24,554[a]
	Lymphocytes (μL)	8645 ± 3427[a]	87,322 ± 67,264[b]	37,865 ± 15,461[a]
	Monocytes (μL)	465 ± 312[a]	3579 ± 3630[a]	1010 ± 590[a]
	Neutrophils (μL)	3558 ± 1903[a]	38,301 ± 37,083[b]	19,714 ± 10,041[a]
14 days	RBC (x10^6 μL^{-1})	0.22 ± 0.06[a]	0.26 ± 0.07[a]	0.19 ± 0.07[a]
	Thrombocytes (μL)	8775 ± 3304[a]	18,090 ± 5972[b]	9900 ± 4779[a]
	WBC (x10^3 μL^{-1})	70,110 ± 55,595[a]	105,732 ± 54,201[a]	86,526 ± 120,412[a]
	Lymphocytes (μL)	51,254 ± 41,516[a]	71,334 ± 36,074[a]	53,282 ± 66,968[a]
	Monocytes (μL)	1318 ± 1360[a]	1626 ± 699[a]	865 ± 1204[a]
	Neutrophils (μL)	17,538 ± 13,449[a]	32,770 ± 17,851[a]	32,378 ± 52,354[a]
21 days	RBC (x10^6 μL^{-1})	0.23 ± 0.05[a]	0.22 ± 0.04[a]	0.23 ± 0.13[a]
	Thrombocytes (μL)	15,235 ± 5444[a]	13,050 ± 3462[a]	14,040 ± 4636[a]
	WBC (x10^3 μL^{-1})	30,188 ± 16,152[a]	56,484 ± 31,953[a]	65,574 ± 34,321[a]
	Lymphocytes (μL)	18,631 ± 5065[a]	40,223 ± 24,863[a]	39,791 ± 21,170[a]
	Monocytes (μL)	495 ± 387[a]	631 ± 298[a]	655 ± 343[a]
	Neutrophils (μL)	11,062 ± 11,703[a]	15,628 ± 6877[a]	25,126 ± 14,804[a]

RBC = Red Blood Cell; WBC = White Blood Cell. Different letters (a or b) in same line indicate differences according to the Dunnett test ($p < 0.05$).

ivermectin leading to possible alteration in Myosin-Vb function, which can have implications in the intestinal epidermal integrity.

3.3. Hematology assays

Hematology showed a statistic no significant alteration in blood cells counts for 0.22 and 0.86 mg/kg at days 7, 14 and 21 after administration (Table 1) for the majority of parameters. An observation is made for the 0.86 mg/kg dose at day 7, where the average of RBC decreased to about the half value found for the control, concomitant with average increase of WBC. For the 0.22 mg/kg at the same day it was also observed significant increase ($p < 0.05$) for WBC, lymphocytes and neutrophils. These changings may also be related to the increased variations and certain abnormalities in the numbers of the different parameters measured, suggesting that ivermectin induced metabolic stress in the fish [39, 40].

These premises my have been confirmed in analyzing the results for the ivermectin overdose (Table 2) where, although the blood collection was performed shortly after administration, the average RBC number equally decreased with an increase of average of WBC, suggesting an initial response to the ivermectin high doses. However, it is further reported that, when in contact with drugs and other types of contaminants, fish have tendency to activate erythropoiesis for its recovery over time [41]. The recovery is actually shown in Table 1 at days 14 and 21, when RBC number was more similar to the control for both concentrations, while WBC still showed certain increased variation, but with a time tendency to equalize to the control.

The safety of ivermectin doses administration to humans is not established. Recent studies have concluded that the safety depends largely on type and severity of infection and immune status of the patient [42]. The usual recommended dose is 0.15 mg/kg as anthelmintic. Higher doses as 0.2 and 0.4 mg/kg have been approved for the treatment of strongyloidiasis and scabies [43]. Doses up to 0.8 mg/kg have been tested in clinical trials for the treatment of onchocerciasis and presented good safety [44]. However, none of the studies provided histological or hematological data. In the present study we applied similar doses, *i.e.*, 0.22 and 0.86 mg/kg. Despite that results described for fish cannot be directly extrapolated to human, our study evidences the safety of the high doses in terms of histologic and hematologic evaluations in an animal model after oral administration. A

remark is given to the extremely high dose of 170 mg/kg, causing some alteration in Myosin-Vb of enterocytes, which is worth of further investigation.

4. Conclusion

In drug repurposing, besides effective pharmacological action, the tolerability and safety of the drug and its dosage need to be known. The majority of safety and pharmacokinetic data on oral administrated ivermectin are from doses of 0.15–0.20 mg/kg. This study provided histologic and hematologic information for higher doses using *Corydoras* fish as animal model. High doses of 0.22 and 0.86 mg/kg were not harmful to the intestinal tissues of the animal model neither affected the blood cells counting in general. The overdose of 170 mg/kg was demonstrated to affect Myosin-Vb, which can have implications in intestinal epidermal integrity. The suitable knowledge of the safety of ivermectin higher doses, which offers likely benefits in the prevention of the emergence of drug resistance besides prospecting the potentiality of the drug for new and emergent applications as drug repurposing, is for these reasons essential. Thereby, this study contributes with new information concerning higher dosage, which can be of supporting matter for studies of the drug resistance and for the drug repositioning as an alternative for new therapeutic applications.

Table 2. Blood cells parameters of *Corydoras schwartzi* after administration of overdose of 170 mg/kg ivermectin compared to the control. Data are expressed as mean ± standard deviation.

Parameters	Control	Ivermectin 170 mg/kg
RBC (x10^6 μL^{-1})	0.21 ± 0.05[a]	0.16 ± 0.09[a]
Thrombocytes (μL)	13,830 ± 6937[a]	13,050 ± 8612[a]
WBC (x10^3 μL^{-1})	35,808 ± 45,075[a]	54,276 ± 56,379[a]
Lymphocytes (μL)	25,736 ± 33,612[a]	42,435 ± 46,836[a]
Monocytes (μL)	795 ± 987[a]	629 ± 577[a]
Neutrophils (μL)	9287 ± 10,948[a]	11,332 ± 10,929[a]

RBC = Red Blood Cell; WBC = White Blood Cell. Different letters in same line (a or b) indicate differences according to the t-test ($p < 0.05$).

Declarations

Data availability statement

Data will be made available on request.

Declaration of interests statement

The authors declare no conflict of interest.

Additional information

Supplementary content related to this article has been published online at https://doi.org/10.1016/j.heliyon.2020.e05820.

References

[1] M. Antoszczak, A. Markowska, J. Markowska, A. Huczynski, Old wine in new bottles: drug repurposing in oncology, Eur. J. Pharmacol. 866 (2020) 172784.

[2] S. Pushpakom, F. Iorio, P. Eyers, et al., Drug repurposing: progress, challenges and recommendations, Nat. Rev. Drug Discov. 18 (2019) 41–58.

[3] L. Caly, J.D. Druce, M.G. Catton, D.A. Jans, K.M. Wagstaff, The FDA-approved drug ivermectin inhibits the replication of SARS-CoV-2 in vitro, Antivir. Res. 178 (2020) 104787.

[4] L. Jin, X. Feng, H. Rong, et al., The antiparasitic drug ivermectin is a novel FXR ligand that regulates metabolism, Nat. Commun. 4 (2013) 1937.

[5] M. Juarez, A. Schcolnik-Cabrera, A. Duenas-Gonzalez, The multitargeted drug ivermectin: from an antiparasitic agent to a repositioned cancer drug, Am. J. Canc. Res. 8 (2018) 317–331.

[6] F. Heidary, R. Gharebaghi, Ivermectin: a systematic review from antiviral effects to COVID-19 complementary regimen, J. Antibiot. (Tokyo) (2020).

[7] V.A. Drinyaev, V.A. Mosin, E.B. Kruglyak, et al., Antitumor effect of avermectins, Eur. J. Pharmacol. 501 (2004) 19–23.

[8] A. Didier, F. Loor, The abamectin derivative ivermectin is a potent P-glycoprotein inhibitor, Anti Canc. Drugs 7 (1996) 745–751.

[9] A. Crump, Ivermectin: enigmatic multifaceted 'wonder' drug continues to surprise and exceed expectations, J. Antibiot. (Tokyo) 70 (2017) 495–505.

[10] S.H. Bai, S. Ogbourne, Eco-toxicological effects of the avermectin family with a focus on abamectin and ivermectin, Chemosphere 154 (2016) 204–214.

[11] M. Navarro, D. Camprubi, A. Requena-Méndez, et al., Safety of high-dose ivermectin: a systematic review and meta-analysis, J. Antimicrob. Chemother. 75 (2020) 827–834.

[12] C.D. Enk, Onchocerciasis: river blindness, Clin. Dermatol. 24 (2006) 176–180.

[13] G. De Sole, J. Remme, K. Awadzi, S. Accorsi, E.S. Alley, O. Ba, K.Y. Dadzie, J. Giese, M. Karam, F.M. Keita, Adverse reactions after large-scale treatment of onchocerciasis with ivermectin: combined results from eight community trials, Bull. World Health Organ. 67 (1989) 707–719.

[14] A.C.M.F. Patta, P.D. Mathews, R.R.M. Madrid, et al., Polyionic complexes of chitosan-*N*-arginine with alginate as pH responsive and mucoadhesive particles for oral drug delivery applications, Int. J. Biol. Macromol. 148 (2020) 550–564.

[15] F.M. Costa, A.D.P. Netto, Development and application of methods for the determination of ivermectin in veterinarian medications, Quim. Nova 35 (2012) 616–622.

[16] P.D. Mathews, A.C.M.F. Patta, J.V. Gonçalves, et al., Targeted drug delivery and treatment of endoparasites with biocompatible particles of pH-responsive structure, Biomacromolecules 19 (2018) 499–510.

[17] https://www.sciencedirect.com/science/article/pii/S0141813019381401?dgcid=r ss_sd_all.

[18] L.A.K.A. Inoue, P.O. Maciel, E.G. Affonso, C.L. Boijink, M. Tavares-Dias, Growth, parasitic infection and hematology in *Colossoma macropomum* Cuvier, 1818 fed diets containing *Allium sativum*, J. Appl. Ichthyol. 32 (2016) 901–905.

[19] M. Tavares-Dias, F.R. Moraes, Caracteristicas hematologicas da Tilapia rendalli Boulenger, 1896 (Osteichthyes: Cichlidae) capturada em "Pesque-Pague" de Franca, Sao Paulo, Bras. Biosci. J. 19 (2003) 103–110.

[20] M. Tavares-Dias, F.R. Moraes, Morphological, cytochemical, and ultrastructural study of thrombocytes and leukocytes in Neotropical fish, Brycon orbignyanus Valenciennes, 1850 (Characidae, Bryconinae), J. Submicr. Cytol. Pathol. 38 (2006) 209–215.

[21] P.D. Mathews, A.C.M.F. Patta, G.S. Gama, O. Mertins, Infestation by Ergasilus coatiarus (Copepoda: Ergasilidae) in two Amazonian cichlids with new host record from Peru: an ectoparasites natural control approach, Comptes Rendus Biol. 341 (2018) 16–19.

[22] N.L.S. Rivadeneyra, O. Mertins, R.C. Cuadros, et al., Histopathology associated with infection by *Procamallanus* (*Spirocamallanus) inopinatus* (Nematoda) in farmed *Brycon cephalus* (Characiformes) from Peru: a potential fish health problem, Aquacult. Int. 28 (2020) 449–461.

[23] M.S. Pinky, A.K. Mittal, Glycoproteins in the epithelium of lips and associated structures of a hill stream fish Garra lamta (Cyprinidae, Cypriniformes): a histochemical investigation, Anat. Histol. Embryol. 37 (2008) 101–113.

[24] F. Cartón-García, A.W. Overeem, R. Nieto, et al., Myo5b knockout mice as a model of microvillus inclusion disease, Sci. Rep. 5 (2015) 12312.

[25] P.D. Mathews, O. Mertins, Dispersion of chitosan in liquid crystalline lamellar phase: production of biofriendly hydrogel of nanocubic topology, Carbohydr. Polym. 157 (2017) 850–857.

[26] H. Cheng, S. Huang, G. Huang, Design and application of oral colon administration system, J. Enzym. Inhib. Med. Chem. 34 (2019) 1590–1596.

[27] N. Kavitha, T.P. Karunya, S. Kanchana, et al., Formulation of alginate based hydrogel from brown seaweed, *Turbinaria conoides* for biomedical applications, Heliyon 5 (2019), e02916.

[28] G. Rydzek, A. Pakdel, A. Witecka, et al., pH-responsive saloplastics based on weak polyelectrolytes: from molecular processes to material scale properties, Macromolecules 51 (2018) 4424–4434.

[29] F. Sciortino, S.H. Mir, A. Pakdel, et al., Saloplastics as multiresponsive ion exchange reservoirs and catalyst supports, J. Math. Chem. A 8 (2020) 17713–17724.

[30] S.S. Pony, C.C. Wang, L.C. Fritz, Studies on the mechanisms of action of avermectin B_{1a}: stimulation of release of gamma amino butyric acid from brain synaptosomes, J. Neurochem. 34 (1980) 351–358.

[31] C.E. Thoeni, G.F. Vogel, I. Tancevski, et al., Microvillus inclusion disease: loss of Myosin Vb disrupts intracellular traffic and cell polarity, Traffic 15 (2014) 22–42.

[32] L.A. Lapierre, R. Kumar, C.M. Hales, et al., Myosin Vb is associated with plasma membrane recycling systems, Mol. Biol. Cell 12 (2001) 1843–1857.

[33] C.M. Hales, J.P. Vaerman, J.R. Goldenring, Rab11 family interacting protein 2 associates with Myosin Vb and regulates plasma membrane recycling, J. Biol. Chem. 277 (2002) 50415–50421.

[34] J.T. Roland, D.M. Bryant, A. Datta, A. Itzen, K.E. Mostov, J.R. Goldenring, Rab GTPase-Myo5B complexes control membrane recycling and epithelial polarization, Proc. Natl. Acad. Sci. U.S.A. 108 (2011) 2789–2794.

[35] H.S. Dhekne, N.H. Hsiao, P. Roelofs, et al., Myosin Vb and Rab11a regulate phosphorylation of ezrin in enterocytes, J. Cell Sci. 127 (2014) 1007–1017.

[36] K. Schneeberger, G. Vogel, H. Teunissen, et al., An inducible mouse model for microvillus inclusion disease reveals a role for myosin Vb in apical and basolateral trafficking, Proc. Natl. Acad. Sci. U.S.A. 112 (2015) 12408–12413.

[37] T. Sobajima, S.I. Yoshimura, T. Iwano, et al., Rab11a is required for apical protein localization in the intestine, Biol. Open 4 (2014) 86–94.

[38] M. Reynier, S. Allart, D. Goudounèche, et al., The actin-based motor Myosin Vb is crucial to maintain epidermal barrier integrity, J. Invest. Dermatol. 139 (2019) 1430–1438.

[39] D. Hemalatha, N. Bojan, R. Basuvannan, et al., DNA damage and physiological responses in an indian major carp Labeo Rohita exposed to an antimicrobial agent triclosan, Fish Physiol. Biochem. 45 (2019) 1463–1484.

[40] E.O. Ogueji, C.D. Nwani, C.E. Mbah, F.N. Nweke, Acute hematological toxicity of ivermectin to juvenile Clarias gariepinus, Toxicol. Environ. Chem. 101 (2019) 300–314.

[41] M.A. Burgos-Aceves, L. Lionetti, C. Faggio, Multidisciplinary haematology as prognostic device in environmental and xenobiotic stress-induced response in fish, Sci. Total Environ. 670 (2019) 1170–1183.

[42] P.J. Budge, C. Herbert, B.J. Andersen, et al., Adverse events following single dose treatment of lymphatic filariasis: observations from a review of the literature, PLoS Neglected Trop. Dis. 12 (2018), e0006454.

[43] C. Chaccour, N.R. Rabinovich, Ivermectin to reduce malaria transmission III. Considerations regarding regulatory and policy pathways, Malar. J. 16 (2017) 162.

[44] K. Awadzi, S.K. Attah, E.T. Addy, et al., The effects of high-dose ivermectin regimens on Onchocerca volvulus in onchocerciasis patients, Trans. R. Soc. Trop. Med. Hyg. 93 (1999) 189–194.